Codebook Based Beamforming and Multiuser Scheduling Scheme for mmWave Outdoor Cellular Systems in the 28, 38 and 60GHz Bands

Djamal E. Berraki, Simon M. D. Armour and Andrew R. Nix
Communication Systems & Networks, University of Bristol
Merchants Ventures Building, Woodland Road, BS8 1TJ, Bristol UK
Email: {d.berraki, simon.armour, andy.nix}@bris.ac.uk

***Abstract*—In this paper a 3D ray tracing tool is developed for mmWave outdoor environments. Coverage analysis and system performance is performed for a small cell system at 60GHz. Peak throughputs beyond 3Gbps and cell edge throughputs in excess of 500Mbps are demonstrated at 98% of the mobile test locations. Analogue codebook based beamforming is applied. The analysis of the statistical angular spread at the mobiles is shown to be clustered; leading to many users selecting the similar analogue beamforming code which results is high levels of co-channel interference. It is often assumed that the use of analogue beamforming implies a single beam pattern pointing in a specific direction to support a single user. In this case users that cannot be spatially separated must be scheduled in different time slots. However, due to the clustered aspect of the users' angle spreads, those with the same beam code can still be scheduled in the same time slot using different frequency channels via a single RF chain. The paper analyses a scheduling scheme based on this concept. The same scheduling scheme is applied to systems operating at 28, 38 and 60GHz where different numbers of frequency channels are available. Different user densities and street scenarios are studied. The 60GHz scheme make use of 4 frequency channels and is shown to double the system throughput compared to operation at 28GHz band using a single frequency channel. Finally, the optimal number of RF chains required at the base station is analysed. This is shown to be a critical design issue for mmWave cellular systems.**

Keywords—Beamforming; mmWave; cellular systems; Co-Channel Interference; Scheduling algorithm; 5G; Coverage performance

I. INTRODUCTION

The data throughput in cellular systems is expected to rise substantially within the next decade [1]. One possible approach to meet this demand is to deploy complex spectrally efficient systems that explore multi antenna architectures in the sub 6 GHz bands. This solution offers limited improvements and will only ease the high demand on user throughputs for a short period of time [2]. One promising alternative is to migrate to higher frequencies, where abundant spectrum is available. At mmWave frequencies user bandwidths of 1-2GHz are available and simple system architectures can deliver very high peak data rates. Combining mmWave systems with cell densification enables substantial system capacity increases with unprecedented cell edge data rates. The mmWave bands that have attracted particular interest are the LMDS bands at 28GHz, 38GHz and the V-band at 60GHz, where 1GHz, 2GHz and 7GHz of bandwidth is available respectively [3]. Assuming a bandwidth of the order of 1GHz, 1, 2 and 7 channel are possible in the three bands respectively.

Due to the unique characteristics of mmWave channel propagation, the cellular system requires radical rethinking. The mmWave small cell system is expected to be a mesh self-organising network, where backhaul and mobile access use the same platform [2]. 5G mmWave systems should aim for individual users to experience peak rates of a several Gbps; with a minimum cell edge throughput of 100Mbps and sub-ms latency. Due to the large bandwidths involved, Gbps rates require high energy efficiency to preserve battery life [4].

In order to meet the pathloss constraints and coverage requirements, large antenna arrays should be employed at the base station. 2 dimensional arrays of typically 8x8 elements or more should be deployed to facilitate considerable spatial frequency reuse. The small form factor of RF and antenna components at mmWave frequencies facilitates the implementation of such large arrays in a compact form factor at the BS, as well as smaller arrays at the terminals [5]. Ideally, full digital beamforming would be implemented for multi antenna systems, where each antenna is equipped with its own RF chain and ADC/DAC converters. However as GHz sampling rates are required, the cost of such architecture (and the high associated power consumption) suggests the use of RF beamforming. Here, a single RF chain lies behind the entire antenna array [6]. For practical reasons, codebook (CB) based beamforming is preferred, where the BS scans through a beam pattern dictionary to identify the best beamforming pattern pair for transmission/reception. Several codebook based beamforming methods are proposed in [7][8]. In this study the codebook proposed in the IEEE 802.15.3c is adopted [7]. If the codebook length is twice as long as the number of antenna elements, this guarantees a maximum of 1dB fluctuation in the antenna gain in all possible directions.

Although adopting an analogue beamforming architecture provides a simple and relatively cheap solution, only a single beam pointing towards a specific direction at a specific time is generated. For this reason, most current research assumes that analogue beamforming with a single RF chain can only support a single user at a given time; hence STDMA based scheduling is proposed for mmWave outdoor systems. However, this paper shows that for a small cell street level deployment, many users share the same preferred beamforming codebook entry. This is due to the clustered distribution of users and the restrained angle spread caused by the street level propagation environment. Therefore, users with the same code can be scheduled in different frequency channels subject to channel availability and use the same beam in the same time slot. This enables users with high co-channel interference to be scheduled in different frequency channels in the same time slot. A combination of space–frequency and time multiple access is evaluated here. Interfering users confined to the same space frame (this can be the same codebook entry or a group of codes where the level of

978-1-4799-7470-2/14/$31.00 ©2014 IEEE

interference is unacceptable, for example due to pattern overlap) are assigned different frequency channels while sharing the same RF chain and analogue beam. The proposed scheme is compared to a spatial reuse scheme based on exclusive regions as in [9] [10], where interfering users can only be scheduled in different time slots. Other scheduling schemes at mmWave frequencies that implement interference cancellation are based on digital or hybrid architectures [11] [12], or require very fine phase control of the antennas as well as assuming the availability of Direction of Departure (DoD) information.

This paper examines the coverage statistics of a 5G network deployed in a generic urban environment in the 60GHz band. An analysis of the statistical distribution of users within the environment is performed. A new scheduling scheme is presented that combines STDMA with multi frequency channels to take advantage of users operating with same selected beam. Finally, analysis of the number of RF chains required for optimal performance of the base station is performed.

II. Simulation Setup

A. System and Channel Models

A 3D Ray tracer for a generic outdoor environment was developed to simulate access via mmWaves. The base stations are fixed on lampposts at a height of 6m. Fig. 1 shows a representation of the outdoor scenario where the number of streets and intersections is variable (here 4 intersections are shown). The trees are positioned on the pavements and the induced attenuation is given by an empirical formula [13]

$$L = 0.2\, f^{0.3} R^{0.6}\ [\text{dB}] \qquad (1)$$

where f is the frequency in MHz, and R is the depth of foliage in metres. For a tree dimension of 6m, the foliage attenuation is 12.6, 13.9 and 16.0dB at 28, 38 and 60GHz respectively.

The 3D ray tracer provides accurate space-time-polarisation characteristics for the propagation channel and supports beamforming for steerable antenna arrays. A Uniform Rectangular Array ($M_x \times M_z$) antenna model is adopted for the base station and the end user with its gain at angle point (θ, φ) given by:

$$D_{BS}(\theta,\varphi) = \left\| \sum_{m_x=0}^{M_x-1} \sum_{m_z=0}^{M_z-1} W_{m_x m_z} \cdot e^{j.(\omega_x m_x + \omega_z m_z)} \right\| \qquad (2)$$

where $\omega_x = 2\pi \left(\frac{d}{\lambda}\right) \sin\varphi \cos\theta$ and $\omega_z = 2\pi \left(\frac{d}{\lambda}\right) \sin\varphi \sin\theta$.

To account for the time varying propagation channel, a Random Waypoint model was adopted for the user movements in the environment. Two scenarios are possible, users walking on the sidewalks and users occupying the whole street. The latter simulated a dense car free city centre. The human body shadowing model is given in [14]. A diffuse scatter model is also implemented for more realistic channel realisations [14]. Table I summarises the key parameters used in the simulations.

TABLE I. Environment and Antenna Simulation Parameters

Parameters	Value
BS position (Tx1)	$[x_t, y_t, 6]$ m,
Street dimensions (LxWxH)	200x 20x8 m
Transmit power	15 dBm
Noise figure	7 dB
Implementation loss	5 dB
Bandwidth	1.08 GHz
Number of antenna elements at BS	8x8
Number of antenna elements at user	4x4
Average 3dB Beamwidth Base station	13°
Frequency carrier	60,38,28GHz

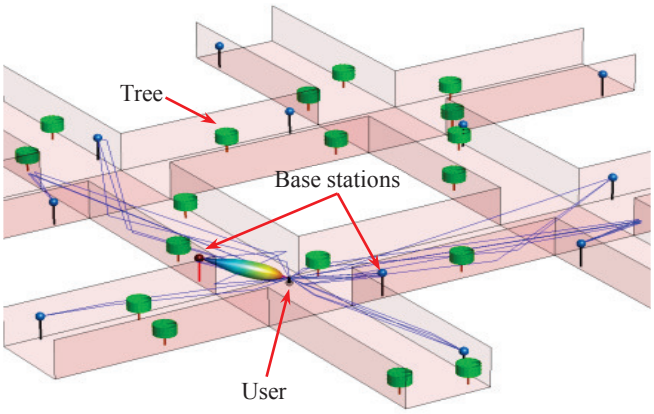

Fig. 1. 3D ray tracing for an outdoor cellular system (4 intersections).

B. Link-level Abstraction Technique

For link level analysis, the system throughput was estimated using a state-of-the-art Received Bit Mutual Information Rate (RBIR) abstraction technique that is fully described in [15] and extensively used in [16]. This approach can be used as an alternative to bit-accurate PHY layer simulation which becomes time prohibitive when applied to system level (multi-user) applications with large combinations of MCS mode, antenna type and orientations [17].

C. Code-book Based Beamforming

An effective way of beamforming is to apply one of a predefined set of beamforming codes to the antenna elements. Following the guidelines of the IEEE 802.15.3c standard [18], the codebook adopted is given by the weights applied to the antenna elements W

$$W(m_x, m_z, k_x, k_z) = j^{\text{fix}\left\{\frac{m_x \times mod[k_x + (K_x/2), K_x]}{K_x/4}\right\} + \text{fix}\left\{\frac{m_z \times mod[k_z + (K_z/2), K_z]}{K_z/4}\right\}}$$

Where fix{} is a function that rounds towards zero, $k_i = 0{:}\,K_i - 1$ represents the index of code k_i in dimension $i = [x, z]$, and K_i is the length of the codebook $K_i \geq M_i$ in dimension i, and $M_x \times M_z$ is the size of the antenna array with $m_i = 0{:}\,M_i - 1$. The total codebook size is given by $K_x \times K_z$. For a maximum fluctuation of 1dB in the achieved gain over all angle point covered by the codebook, the parameter K_i requires to be equal to $2 \times M_i$ generating a large codebook size of $4 \times M_x \times M_z$. In this work a reasonable codebook size of $M_x \times M_z$ is adopted which is associated with a maximum 3.9dBi gain fluctuation.

Fig. 2 shows to the left beam pattern of a patch slot antenna (4×4) for the end user and to the right the 64 entries of the codebook associated with this antenna.

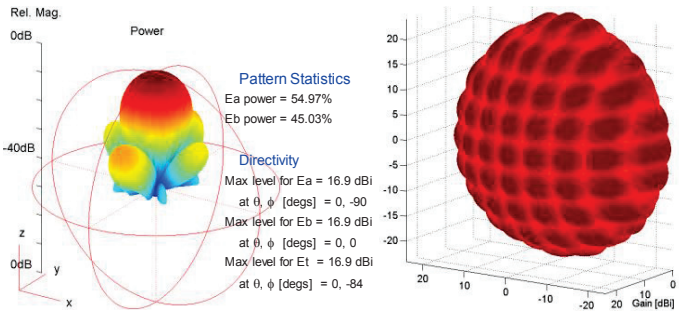

Fig. 2. Right: Beam pattern of user antenna; Left: 802.15.3c codebook with 64 entrees for an antenna array (4x4).

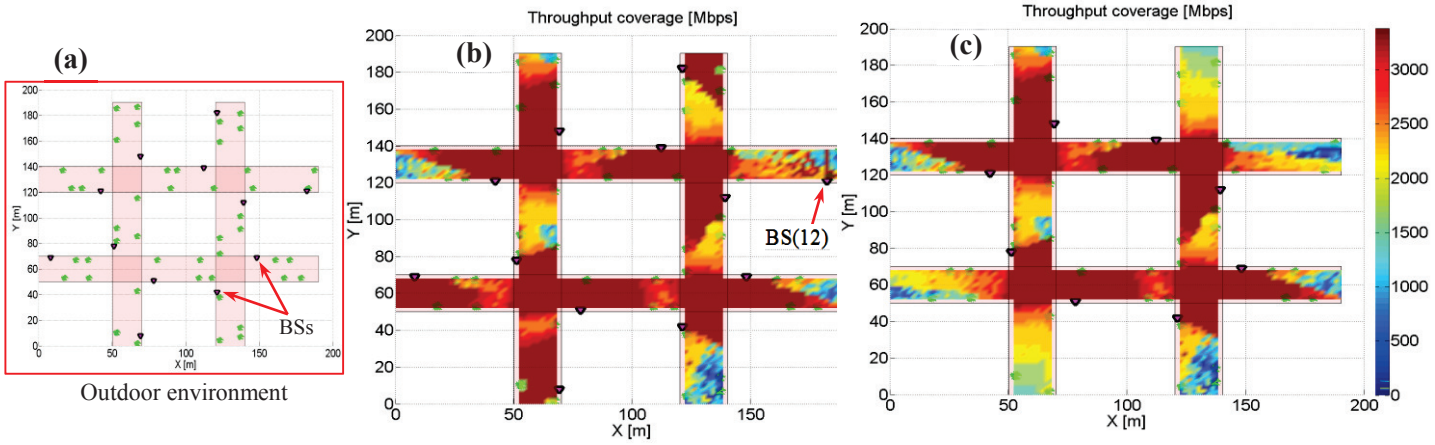

Fig. 3. Outdoor coverage for 12 and 8 base stations in a 200x200m^2 environment.

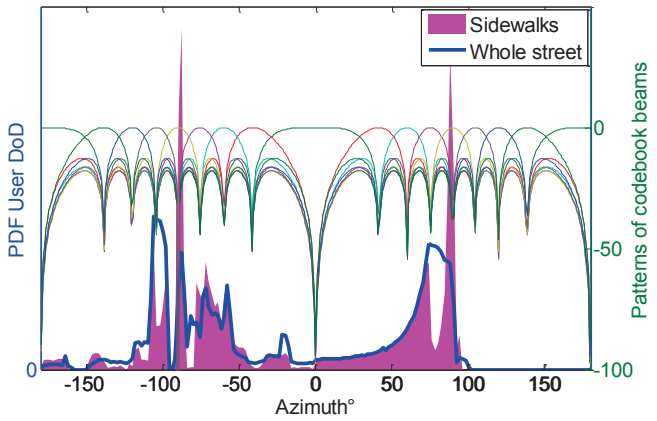

Fig. 4. Distribution of the azimuth angle of the strongest ray for users occupying the sidewalks and the whole street. The beam patterns generated by the 802.15.3c codebook are also plotted in the azimuth plane.

III. System Performance Analysis

A. Environment Analysis:Angular Characterisation

Statistical angular characteristics of the propagation channel were calculated from ray tracing simulations. The probability density function of the strongest ray is plotted in Fig. 4. The beam patterns in the azimuth plain generated from the 3c codebook are drawn in the same figure. It can be observed that the PDF of the azimuth of the users' DoD is not uniformly distributed but clustered within a confined azimuth spread around -90° and +90° for both scenarios: users occupying the whole street and users constrained to the sidewalks. It can be observed that the BS would select the same beam pattern for many users; this is particularly true for the sidewalk scenario. Since the BS can only generate a single beam at any given time for a given RF chain, we propose that users that belong to the same exclusive region (as defined by a specific beam) are scheduled in the same time slot and beam pattern but in different frequency channels.

B. Coverage Analysis

In this section, the outdoor coverage performance for the scenario shown in Fig. 3-(a) is analysed. The coverage map of the outdoor environment in the 60GHz band is depicted in Fig.3. Two scenarios are shown with 8 and 12 BSs. These are represented by triangles in Fig. 3. It can be seen that the foliage introduces considerable blockage and consequently this has a significant effect on the achieved throughput in some regions. This suggests that when planning the BS deployment, special care should be taken to position the BS in open spaces, well away from foliage, to increase the probability of users being in LOS conditions. As an example, BS(12) in Fig. 3-(a) is positioned on a lamppost at a height of 6m just above a tree (height of 5.5m). This led to poor area coverage around BS(12).

If a single BS is considered in the scenario, the achieved throughput of all the LOS positions within a 100m radius around the BS is shown in Fig. 5. Here it can be observed that a minimum guaranteed throughput of 1Gbps and an average throughput of 2.7Gbps are realised in LOS conditions. On the other hand, only 20% of the NLOS user locations within the BS coverage area (100m radius) achieve a throughput in excess of 500Mbps. This is shown in the NLOS throughput CDF for a single BS in Fig.6. This means that a single deployed BS can only provide coverage for up to 100m for LOS scenarios and would not be able to support NLOS locations at this maximum distance. To provide better reliability, cooperative multi-adjacent small cells must be deployed as shown in Fig. 3. The throughput CDF for a total number of deployed BS of 12 and 8 is shown in Fig.6. A peak throughput of 3.35Gbps and average throughputs of 2.9Gbps and 2.7Gbps are observed for the 12 and 8 BSs scenarios respectively. The cell edge throughput (at 5%) is over 1Gbps with a throughput over 500Mbps at 98% and 99% of user locations for the 12 and 8 BS scenarios respectively. This demonstrates the ability of mmWave small cell systems to meet the 5G cell edge requirements of a minimum of 100Mbps.

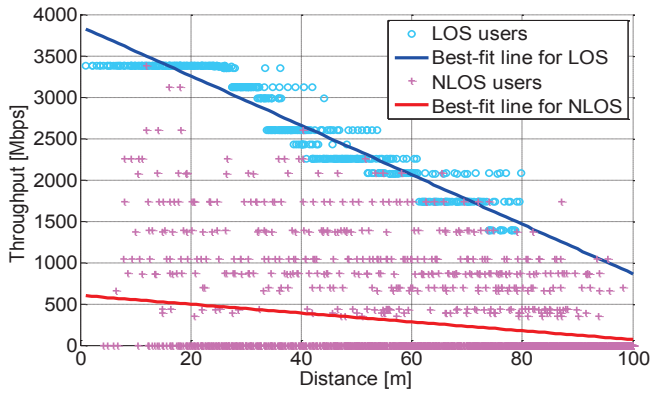

Fig. 5. Achieved throughput vs. distance for users around the base station 1.

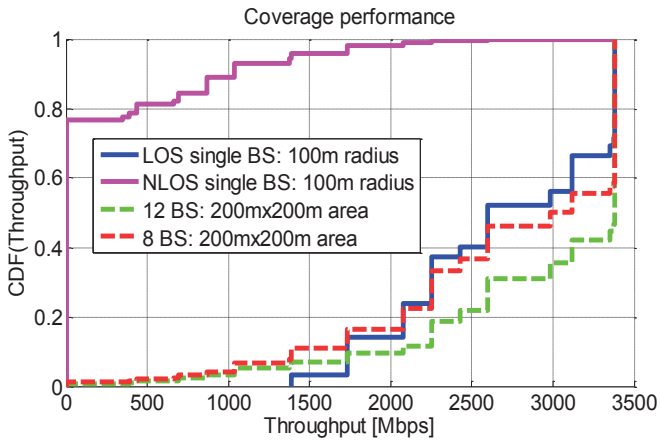

Fig. 6. Achieved throughput vs. distance for users within 100m of base station 1.

IV. MULTIUSER SCHEDULING SCHEME

In this section, the proposed scheduling scheme is described and analysed. We define the CCI matrix as the matrix that identifies the presence or absence of interference between each pair of users, U_i and U_j where the position of ones identifies the interfering users

$$CCI_{mat}(U_i, U_j) = \begin{cases} 1 \ if \ |C_i - C_j| > C_{ref} \\ 0 \ if \ |C_i - C_j| \leq C_{ref} \end{cases} \quad (3)$$

where C_i and C_j are the index of the codes selected in the codebook for users U_i and U_j. C_{ref} is an integer constant can take values from 0 to 2, which represents the maximum number of index difference between the two users that are considered interfering with each other. If C_{ref} is set to 0, two users are not considered as interfering with each other unless they select similar codes. Whereas if C_{ref} is set very large, then the users might be shown as interfering with each other in the CCI_{mat} matrix while in reality they are causing negligible disturbance. Here C_{ref} is set to "0" for $K_i = M_i$ (User isolation who select adjacent beams varies from 0 to 30dB). All interfering users are allocated different time slots unless they share same beam, in which case they are assigned different frequency channels, subject to spectrum availability.

A. Multiuser Scheduling Scheme Description

The scheduling scheme is processed one time slot at a time. Each time slot T_s accommodates as many non-interfering users as possible in a single frequency channel. The remaining users that causing interference (i.e. share the same beams with previously scheduled users) can then be allocated different frequency channels. By doing so, the time-frequency and space channels are all optimally exploited. The users are processed following a certain priority order (to maximise a certain metric). Users that are not previously scheduled are always prioritised over those previously allocated resource blocs. Once the first time slot is allocated, the following slots are assigned until all users are accommodated. The scheduling algorithm generates the set $S_s(T_s, Ch)$ that includes users $\{U_i, \in S_s(T_s, Ch)\}$ scheduled in the time slot T_s and frequency channel Ch. The CCI_{mat} matrix dictates if two users are interfering with each other or can be scheduled at the same time frame and channel frequency. The scheduling process is described in the following algorithm:

Algorithm

BEGIN:
Initialise: Scheduling slot 1:$S_s(1,1) = \emptyset$,
Time slot $T_s = 1$. Frequency channel $Ch = 1$.
Set priority of users: sort users $\{U_i, i = 1, .., K\}$ (for example by lowest SNR_i) : $P_u^{(1)} = \{U_{p(1)}, .., U_{p(K)}\}$.
List of not scheduled yet users: $L_{NS} = P_u^{(1)} = \{U_{p(i)}, i = 1, .., K\}$.
List of scheduled users: $L_S = \emptyset$.
While $L_{NS} \neq \emptyset$
  For non-scheduled user $U_{p(i)} \in L_{NS}$
    If $U_{p(i)}$ does not interfere with users in $S_s(T_s, 1)$
      Add $U_{p(i)}$: $S_s(T_s, 1) = S_s(T_s, 1) \cup \{U_{p(i)}\}$.
      Update L_{NS}: $L_{NS} = L_{NS} \backslash \{U_{p(i)}\}$,
        L_S: $L_S = L_S \cup \{U_{p(i)}\}$.
    End if
  End for
  For Scheduled user $U_{p(i)} \in L_S$
    If $U_{p(i)}$ does not interfere with users in $S_s(T_s, 1)$
      Add $U_{p(i)}$: $S_s(T_s, 1) = S_s(T_s, 1) \cup \{U_{p(i)}\}$.
    End if
  End for
  For $Ch = 2$ to Ch_{max}
    For user $U_{p(i)} \notin S_s(T_s, :)$
      If $U_{p(i)}$ does not interfere with users in $S_s(T_s, Ch)$
        Add $U_{p(i)}$: $S_s(T_s, Ch) = S_s(T_s, Ch) \cup \{U_{p(i)}\}$.
        If $U_{p(i)} \in L_{NS}$
          Update L_{NS}: $L_{NS} = L_{NS} \backslash \{U_{p(i)}\}$,
            L_S: $L_S = L_S \cup \{U_{p(i)}\}$.
        End if
      End if
    End for
  End for
  $T_s = T_s + 1$.
End while
END;

It is worth mentioning that the priority criterion can be set to satisfy any criterion such as the minimum throughput requirement of applications running at each user. This will permit for example to meet the QoS constraints for certain applications.

To illustrate these operations an example with 6 users u_i $(i = 1{:}\,6)$ is considered. The parameter C_{ref} is set to zero. If the index of the selected beam for each user are set as

$$CB_{index} = \begin{bmatrix} & u1 & u2 & u3 & u4 & u5 & u6 \\ index & 3 & 3 & 10 & 6 & 6 & 6 \end{bmatrix},$$

the CCI_{mat} matrix derived from CB_{index} is given by

$$CCI_{mat} = \begin{bmatrix} & u1 & u2 & u3 & u4 & u5 & u6 \\ u1 & 0 & 1 & 0 & 0 & 0 & 0 \\ u2 & 1 & 0 & 0 & 0 & 0 & 0 \\ u3 & 0 & 0 & 0 & 0 & 0 & 0 \\ u4 & 0 & 0 & 0 & 0 & 1 & 1 \\ u5 & 0 & 0 & 0 & 1 & 0 & 1 \\ u6 & 0 & 0 & 0 & 1 & 1 & 0 \end{bmatrix},$$

Where "1" and "0" represents the presence or absence of interference between two users. Assuming that two frequency channels $Ch1$ and $Ch2$ are available, the scheduling matrix S_s is then given by

$$S_s = \begin{bmatrix} & & u1 & u2 & u3 & u4 & u5 & u6 \\ Ts1 & Ch1 & 1 & 0 & 1 & 1 & 0 & 0 \\ Ts1 & Ch2 & 0 & 1 & 0 & 0 & 1 & 0 \\ Ts2 & Ch1 & 1 & 0 & 1 & 0 & 0 & 1 \\ Ts2 & Ch2 & 0 & 1 & 0 & 1 & 0 & 0 \end{bmatrix},$$

where Ts_i represent time slot i. It can be easily observed that only two time slots are required to accommodate all users. Assuming a superframe structure in the MAC protocol, this pattern is then applied for the whole superframe. As u_1 and u_2 are interfering with each other and using the same beamforming code, they are both scheduled at different frequency channels within the same time slot. The same can be said for u_4, u_5 and u_6 with the exception that only two Channels are available hence the second time slot is required. u_1, u_2 and u_4 are again rescheduled in the second time slot as a matter of optimising the resources. Note that a single user cannot aggregate two frequency channels within the same time slot as 1GHz of bandwidth per user is already a challenge for such systems. It should also be noted that the users can be processed in a certain order to satisfy certain criterion such as minimum throughput requirement or better fairness. This will be the subject of future work.

B. Simulation Results

In this section, the performance of the proposed scheduling scheme is analysed. Situations where users are spatially inseparable are often assumed to be undesired and to cause poor system performance. In this section these same scenarios are shown to boost the system performance. The three bands 28GHz, 38GHz and 60GHz are compared with the assumption that 1, 2 and 4 frequency channels of 1GHz are available in each band respectively. The 28GHz band, although having the smallest channel number, has better propagation characteristics than the 60GHz band. With a single channel, it will be considered as a reference for comparison as it does not provide any improvements from FDMA.

The number of users was set to 15 and 30 in each street to analyse the impact of users' density on interference levels and system performance. For a given number of users, 100 random scenarios were analysed for both sidewalk and whole streets occupancy conditions. Each user is assigned to the base station with the highest achievable SNR. The 8 base stations scenario was assumed. The number of RF chains was set in order to meet the requirements of the BS to accommodate as many users as possible; thus identifying the optimal number of RF chains that should be incorporated in a BS to trade-off between performance and cost. Other simulation parameters are assumed identical to those in section III.

We measure the fairness between users by the Jain's fairness index which takes values between 0 and 1 and evaluate the fairness between all the users competing for allocated channel resources [19]

$$JFI = \left(\sum_{i=1}^{N} R_i(t)\right)^2 / N.\sum_{i=1}^{N}\left(R_i(t)\right)^2 \qquad (4)$$

where R_i represents the data rate achieved by user i.

TABLE II. AVERAGE (USER THROUGHPUT (GBPS)/ FAIRNESS)

Environment	Whole street		Sidewalk	
User density	15	30	15	30
60GHz	1.43 / 0.64	0.76 / 0.44	1.41 / 0.60	0.79 / 0.46
38GHz	0.96 / 0.58	0.58 / 0.41	0.94 / 0.55	0.57 / 0.42
28GHz	0.64 / 0.53	0.34 / 0.34	0.61 / 0.49	0.35 / 0.34

Table II shows the average achieved user throughput and fairness between users for different number of users and street scenarios. Over all, the 60GHz band performs better with over 1 Gbps links for the less dense scenario. For higher numbers of users, the throughput is almost halved for all bands. As users are more clustered in the sidewalk scenario, less throughput per user and fairness is observed. The 60GHz band combined with the proposed scheduling scheme is shown to provide twice as much achievable throughput at the 28GHz band and over 8 times more than the 60GHz band with TDMA scheduling.

Although the throughput per user is reduced in denser scenarios, the overall cell throughput is increased as can be seen in the cell throughput CDF for the 60GHz and 38GHz bands in Fig. 7. The 28GHz band however does not provide any cell throughput improvement which suggests that the BSs are already saturated for a density of 15 users in each street. As expected, the fairness between users is affected by the increase in the number of users which are more likely to interfere with each other.

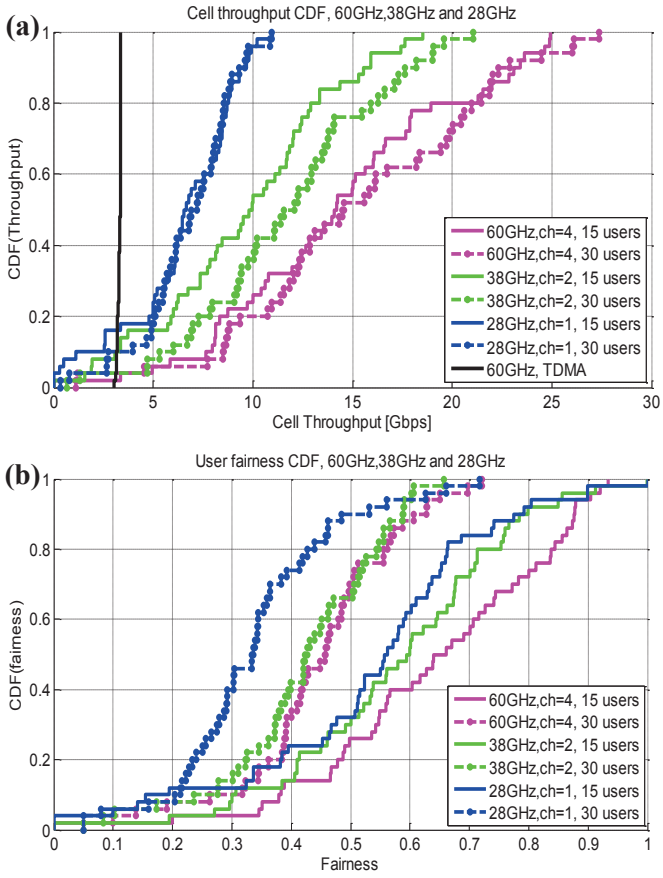

Fig. 7. CDF of cell throughput and JFI for 60GHz, 38GHz&28GHz with different user density of 15&30 per street.

TABLE III. AVERAGE NUMBER OF TIME SLOTS

Environment	Whole street	
User density	15	30
60GHz	2	3
38GHz	3	6
28GHz	6	11

Table III shows the average number of time slots needed to accommodate all the users in the scheduling matrix. Thanks to the large number of frequency channels at 60GHz, the average number of time slots required was 2 for the 15 users case in contrast with 6 for the 28GHz band. 60GHz system manifests more resilience to the increase number of users unlike the

28GHz band where the average number of time slots almost doubled for the denser scenario.

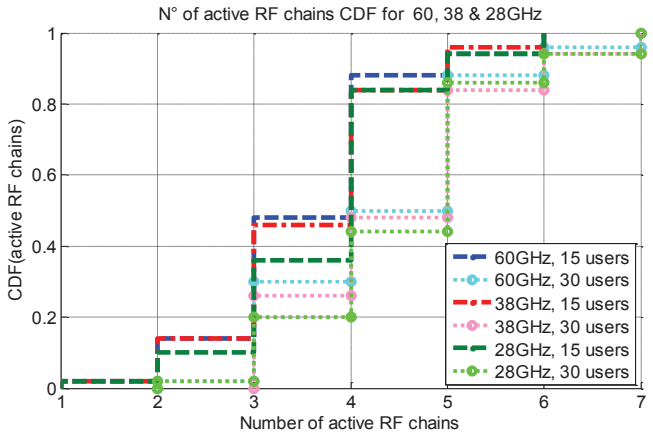

Fig. 8. CDF of number of required RF chains for 60GHz, 38GHz&28GHz with different user density of 15&30 per street.

Fig. 8 represents the CDF of the number of active RF chains at the base stations for the two users' densities. It can be observed from Fig.8 that the CDF curves of the three bands are relatively close to each other for a given user density with slightly less requirements for 60GHz compared with the other frequency bands which is due to the availability of more frequency channels. A maximum number of RF chains of 6 and 7 was respectively required for the lower and higher users' density. In general, the more users in the scenario the more RF chains required at the base stations.

V. Conclusions

This work has presented results from a 3D ray tracing tool for a generic model of an outdoor mmWave system. Coverage analysis for the outdoor mmWave system was performed with foliage effects and for different base station densities. A peak throughput of 3.35Gbps, an average throughput of 2.9Gbps and a cell edge throughput (at 5%) of 1Gbps was demonstrated as feasible for well-planned small-cell deployments.

The statistical angular characteristics of the propagation channel were calculated from ray tracing simulations and these showed the clustered nature of the DoD of users due to the spatial constraints associated with the propagation environment in a street scenario. This led to the conclusion that many users would share the same code for beamforming. Previously, users that select the same beam code were considered to be interferers and recommended to be scheduled at different time slots. Based on the findings of this paper, since analogue codebook-based beamforming is expected to be adopted for mmWave outdoor systems, users that have the same code can be accommodated on different frequency channels while using the same beam pattern and time slot. The proposed scheduling was applied for 60GHz, 38 GHz and 28GHz deployments for different users' densities and street occupancy scenarios. The 60GHz band with 4 frequency channels was shown to achieve twice the performance of the 28GHz band with a single frequency channel. It was also 8 times better than a TDMA scheme. The number of required RF chains was analysed and shown to be a very critical parameter when designing mmWave cellular system. For 80% of the studied scenario, the base stations required at least 6 RF chains for an optimal performance.

References

[1] Cisco Visual Networking Index Mobile Data Traffic Forecast and Methodology, 2012-2017, white paper.

[2] Ghosh, A; Thomas, T.A; Cudak, M.C.; Ratasuk, R.; Moorut, P.; Vook, F.W.; Rappaport, T.S.; MacCartney, G.R.; Sun, S.; Nie, S., "Millimeter Wave Enhanced Local Area Systems: A High Data Rate Approach for Future Wireless Networks," Selected Areas in Communications, IEEE Journal on , vol.PP, no.99, pp.1,1 2014.

[3] Ott, D.; Talwar, S., "Exploring Next Generation Wireless (5G): Transforming the User Experience," *IDF13*, *ACAS002*, 2013.

[4] Andrews, J.G.; Buzzi, S.; Choi, W.; Hanly, S.; Lozano, A; Soong, AC.K.; Zhang, J.C., "What Will 5G Be?," Selected Areas in Communications, IEEE Journal on , vol.PP, no.99, pp.1,1 2014.

[5] Laskar, J.; Pinel, S.; Dawn, D.; Sarkar, S.; Sen, P.; Perunama, B.; Yeh, D.; Barale, F., "60GHz entertainment connectivity solution," *Ultra-Wideband, 2009. ICUWB 2009. IEEE International Conference on*, vol., no., pp.17, 21, 9-11 Sept. 2009.

[6] Nsenga, J.; Bourdoux, A.; Horlin, F., "Mixed Analog/Digital Beamforming for 60 GHz MIMO Frequency Selective Channels," Communications (ICC), 2010 IEEE International Conference on, vol., no., pp.1,6, 23-27 May 2010.

[7] Kishore, R.; Narayan, P.; Kenichi, H.; Kenichi, M.; Sampath, R., "Adaptive Beamforming for 60 GHz Radios: Challenges and Preliminary Solutions". *In ACM mmCom Workshop*, 2010.

[8] Bin, L.; Zheng, Z.; Weixia, Z.; Xuebin, S.; Guanglong, D., "On the Efficient Beam-Forming Training for 60GHz Wireless Personal Area Networks," *IEEE Transactions on Wireless Communications*, no.99, pp.1-12 Feb. 2013.

[9] Jian, Q.; Cai, L.X.; Xuemin, S.; Mark, J.W., "STDMA-based scheduling algorithm for concurrent transmissions in directional millimeter wave networks," *Communications (ICC), 2012 IEEE International Conference on* , vol., no., pp.5221,5225, 10-15 June 2012.

[10] In Keun, S.; Shiwen, M.; Gong, M.X.; Yihan, L., "On frame-based scheduling for directional mmWave WPANs," *INFOCOM, 2012 Proceedings IEEE* , vol., no., pp.2149,2157, 25-30 Mar. 2012.

[11] Alkhateeb, A.; El Ayach, O.; Leus, G.; Heath, R.W., "Hybrid precoding for millimeter wave cellular systems with partial channel knowledge," *Information Theory and Applications Workshop (ITA)*, 2013 , vol., no., pp.1,5, 10-15 Feb. 2013.

[12] Zhiwei ,L.; Xiaoming, P.; Chin, F., "Enhanced beamforming for 60GHz OFDM system with co-channel interference mitigation," Ultra-Wideband (ICUWB), *2011 IEEE International Conference on* , vol., no., pp.29,33, 14-16 Sept. 2011.

[13] Marcus, M.; Pattan, B., "Millimeter wave propagation; spectrum management implications," Microwave Magazine, IEEE , vol.6, no.2, pp.54,62, June 2005.

[14] IEEE 802.11-09/0334r8, "Channel Models for 60 GHz WLAN Systems," 2010-5-20.

[15] Halls, D.; Nix, A.R.; Beach, M.A., "System Level Evaluation of UL and DL Interference in OFDMA," *IEEE WCNC*, May 2011.

[16] Berraki, D.E.; Armour, S.M.D.; Nix A.R., " Polarimetric Filtering for an Enhanced Multi-User 60GHz WPAN System," *IEEE WCNC14*, 6-9 Apr. 2014.

[17] ISO/IEC/IEEE 8802-11:2012/Amd.3:2014(E), vol., no., pp.1,634, March 14 2014.

[18] IEEE Std 802.15.3c-2009 (Amendment to IEEE Std 802.15.3-2003) , vol., no., pp.c1,187, Oct. 12 2009

[19] Jain, R.; Chiu, D.; Hawe, W., "A Quantitative Measure of Fairness and Discrimination for Resource Allocation in Shared Computer Systems", *DEC Research Report TR-301, Digital Equipment Corporation*, Sept. 1984.